

NCAM140 Interacts with the Focal Adhesion Kinase p125^{fa}k and the SRC-related Tyrosine Kinase p59^{fy}n*

(Received for publication, December 17, 1996)

Hilary E. Beggs, Steven C. Baragona, John J. Hemperly‡, and Patricia F. Maness§

From the Department of Biochemistry, School of Medicine, University of North Carolina, Chapel Hill, North Carolina 27599-7260 and the ‡Department of Neurobiology, Becton Dickinson Research Center, Research Triangle Park, North Carolina 27709

Axonal growth cones respond to adhesion molecules and extracellular matrix components by rapid morphological changes and growth rate modification. Neurite outgrowth mediated by the neural cell adhesion molecule (NCAM) requires the *src* family tyrosine kinase p59^{fy}n in nerve growth cones, but the molecular basis for this interaction has not been defined. The NCAM140 isoform, which is found in migrating growth cones, selectively co-immunoprecipitated with p59^{fy}n from non-ionic detergent (Brij 96) extracts of early postnatal mouse cerebellum and transfected rat B35 neuroblastoma and COS-7 cells. p59^{fy}n did not associate significantly with the NCAM180 isoform, which is found at sites of stable neural cell contacts, or with the glycosphosphatidylinositol-linked NCAM120 isoform. pp60^{c-src}, a tyrosine kinase that promotes neurite growth on the neuronal cell adhesion molecule L1, did not interact with any NCAM isoform. Whereas p59^{fy}n was constitutively associated with NCAM140, the focal adhesion kinase p125^{fa}k, a nonreceptor tyrosine kinase known to mediate integrin-dependent signaling, became recruited to the NCAM140-p59^{fy}n complex when cells were reacted with antibodies against the extracellular region of NCAM. Treatment of cells with a soluble NCAM fusion protein or with NCAM antibodies caused a rapid and transient increase in tyrosine phosphorylation of p125^{fa}k and p59^{fy}n. These results suggest that NCAM140 binding interactions at the cell surface induce the assembly of a molecular complex of NCAM140, p125^{fa}k, and p59^{fy}n and activate the catalytic function of these tyrosine kinases, initiating a signaling cascade that may modulate growth cone migration.

Neuronal migration, axon pathfinding, and fasciculation are fundamental processes that underlie the formation of accurate synaptic connections during development. These processes are governed by interactions of cell adhesion molecules, extracellular matrix, and neurotrophic factors with receptors on the neuronal cell surface. How these interactions are integrated and translated biochemically into molecular signals that guide growth cones to their synaptic targets is not well understood.

NCAM,¹ a neural cell adhesion molecule of the immunoglobulin (Ig) superfamily, promotes axon growth, fasciculation, and

cell adhesion by homophilic and heterophilic interactions (1). NCAM has a complex expression pattern due to alternative splicing, developmental regulation, and posttranslational processing, producing a number of isoforms. Alternative splicing of a single gene results in three major NCAM isoforms as follows: transmembrane forms of 140 and 180 kDa, and a 120-kDa glycosphosphatidylinositol (GPI)-linked isoform (2). The cytoplasmic domains of the transmembrane isoforms lack catalytic activity but may mediate interactions with intracellular cytoskeletal and signaling molecules. NCAM180 is identical to NCAM140 except for a 261-amino acid insert in the cytoplasmic domain (2). This insert confers the potential for interaction with spectrin and reduces lateral mobility of NCAM in the plasma membrane (3). NCAM140 is present in free, migratory growth cones, whereas NCAM180 is found at sites of cell-cell contact, where it may be involved in stabilization of synapses (3, 4). NCAM120 is present in some neurons but is mainly found in glia (5). All three isoforms can be posttranslationally modified by addition of polysialic acid, a carbohydrate moiety that modulates axon guidance (6, 7). NCAM can also be expressed as an isoform with a 10-amino acid insertion in the 4th Ig domain (VASE isoform), resulting in down-regulation of its axon growth-promoting ability (8–10). NCAM functions in the adult as a modulator of learning, memory, and synaptic plasticity, as NCAM antibodies reduce long term potentiation in rat hippocampal slices (11), and mice with a total NCAM gene knockout have deficits in spatial memory (12). L1, another transmembrane glycoprotein of the Ig superfamily found in growth cones and axons, plays similar roles in adhesion and neurite growth and may also function in learning and memory (11, 13–15).

Stimulation of NCAM or L1 on the cell surface by homophilic binding or by binding of antibodies that recognize extracellular determinants of NCAM or L1 evokes changes in protein tyrosine phosphorylation (16, 17) and other intracellular signaling responses including calcium rise, pH changes, and altered phosphoinositide turnover (18–20). Atashi *et al.* (16) first demonstrated that such “triggering” of NCAM and L1 modulates tyrosine phosphorylation of proteins associated with growth cone membranes, and Klinz *et al.* (17) showed that this occurs by changes in the activities of both tyrosine kinases and tyrosine phosphatases. Studies with tyrosine kinase inhibitors such as genistein have demonstrated positive as well as negative effects of tyrosine phosphorylation on neurite outgrowth (21–24), and mutational studies in *Drosophila* have defined functions for certain transmembrane tyrosine phosphatases in regulating axon guidance (25, 26).

Two members of the *src* family of nonreceptor tyrosine ki-

* This research was supported by National Institutes of Health Grant NS26620 (to P. F. M.). The costs of publication of this article were defrayed in part by the payment of page charges. This article must therefore be hereby marked “advertisement” in accordance with 18 U.S.C. Section 1734 solely to indicate this fact.

§ To whom correspondence should be addressed. Tel.: 919-966-2323; Fax: 919-966-2852; E-mail: srclab@med.unc.edu email.

¹ The abbreviations used are: NCAM, neural cell adhesion molecule; GPI, glycosphosphatidylinositol; CHAPS, 3-[(3-cholamidopropyl)dimethyl-

ylammonio]-1-propanesulfonic acid; mAb, monoclonal antibody; pAb, polyclonal antibody; PAGE, polyacrylamide gel electrophoresis; PND, postnatal day.

nases, $p59^{fyn}$ and $pp60^{c-src}$, act as positive regulators of neurite growth (27, 28). During the major period of neuronal process outgrowth, these kinases are widely expressed on many axonal tracts, where they are localized to the plasma membrane of growth cones and axons (29–31). $p59^{fyn}$ and $pp60^{c-src}$ exhibit a remarkable specificity for stimulating neurite growth on NCAM and L1, respectively. Cerebellar and dorsal root ganglion neurons from *fyn*-minus mice display complete inhibition of NCAM-dependent neurite growth on NCAM140-expressing fibroblast monolayers, whereas *src*-minus and *yes*-minus neurons show unimpaired neurite growth on NCAM (27). On an L1 substrate, neurons from *src*-minus but not *fyn*- or *yes*-minus mice are impaired for neurite outgrowth, although in this case neurite growth is reduced by only 50% (28). These results suggest the existence of separately regulated pathways for NCAM and L1 signaling.

NCAM and L1 signaling pathways appear to be capable of some degree of functional compensation, as *fyn*-minus and *src*-minus mice do not have severe neurological phenotypes. However, the hippocampus of *fyn*-minus mice is mildly affected, showing loosely organized dendrites of CA1 pyramidal cells, increased neuronal number, and blunted long term potentiation (32). Another strain of *fyn*-minus mice displays partially impaired myelination (33). *src*-minus mice show no neurological abnormalities but instead develop osteopetrosis, a bone remodeling disease of osteoclasts (34). Because both NCAM and L1 are coexpressed on many neuroanatomical tracts, the effects of eliminating either $p59^{fyn}$ or $pp60^{c-src}$ might be minimized due to compensation by the other intact adhesion pathway. In support of this possibility, *src/fyn* double mutants show defective axonal growth *in vivo* (35) and die perinatally (36). Such separately regulated adhesion pathways may serve to minimize errors in axonal pathfinding.

A biochemical approach has been undertaken to identify the molecular components of the NCAM signaling pathway. Here it is reported that $p59^{fyn}$ but not $pp60^{c-src}$ associated preferentially with the NCAM140 isoform. In addition the focal adhesion kinase ($p125^{fak}$) (37), a nonreceptor tyrosine kinase that mediates extracellular matrix signaling through integrin receptors, was recruited to the complex by NCAM cross-linking, and both $p125^{fak}$ and $p59^{fyn}$ became rapidly and transiently phosphorylated on tyrosine upon NCAM stimulation. These results suggest that NCAM140, $p125^{fak}$, and $p59^{fyn}$ comprise a functional adhesion signaling complex that may modulate growth cone motility.

EXPERIMENTAL PROCEDURES

Cell Cultures, Antibodies, and NCAM Fusion Protein

Simian COS-7 cells were obtained from the American Type Culture Collection (ATCC, Rockville, MD). Rat B35 neuroblastoma cell lines stably expressing cDNAs encoding NCAM140 or -180 (9) were obtained from the laboratory of Dr. Richard Akeson (Children's Hospital Medical Center, Cincinnati, OH). All cell lines were cultured in Dulbecco's modified Eagle's medium containing 10% fetal calf serum. The following monoclonal (mAb) and polyclonal (pAb) antibodies were used: $p59^{fyn}$ pAb FYN3 (Santa Cruz, CA), $pp60^{c-src}$ mAb 327 (38), NCAM mAbs 14.2 and 16.2 (Becton Dickinson, Inc.), NCAM mAb 5B8 (Developmental Studies Hybridoma Bank, University of Iowa), NCAM mAb 310 (Chemicon International Inc., Temecula, CA), NCAM pAb 1505 (Sigma), $p125^{fak}$ pAbs BC3 and HUB3 (M. Schaller, University of North Carolina; T. Parsons, University of Virginia), phosphotyrosine mAb 4G10 (Upstate Biotechnology Inc., Lake Placid, NY), normal rabbit and mouse IgG (Sigma), and goat anti-rat and anti-mouse IgG (Sigma).

Chinese hamster ovary cells expressing a fusion protein consisting of the entire NCAM extracellular domain fused to the Fc region of human IgG were provided by Melitta Schachner (Swiss Federal Institute of Technology). The NCAM-Fc protein was isolated from conditioned medium by affinity chromatography using Protein G-Sepharose.

Plasmids, Transfection, and Extract Preparation

The eukaryotic expression vector pcDNA3 containing the human cytomegalovirus promoter was used for all constructs. Plasmid constructs contained full-length cDNA clones encoding the B isoform of mouse $p59^{fyn}$, which is expressed in brain and other tissues (39), the mouse *c-src*⁺ isoform containing a 6-amino acid insert in the SH3 domain (40), the chicken *c-src* isoform lacking that insert (M. Schaller, University of North Carolina), or the rat NCAM140 and NCAM180 isoforms with and without VASE sequences (R. Akeson laboratory, Children's Hospital Medical Center, Cincinnati, OH).

COS-7 or B35 neuroblastoma cells (2×10^6 cells/plate) were transfected to serum-free Opti-MEM (Life Technologies, Inc.) and transfected with indicated plasmid DNA (10 μ g) for 8 h at 37 °C using lipofectamine (Life Technologies, Inc.). Fetal calf serum (10%) was added, and cells were incubated for a further 16 h. Medium was replaced with either Opti-MEM containing 10% fetal calf serum (COS-7 cells) or 0.5% fetal calf serum and 1 mM dibutyl cAMP to induce neuronal differentiation (B35 cells). Cells were incubated for a further 24 h before lysis or NCAM cross-linking. For lysis the medium was removed and cells were incubated for 5 min at 4 °C with Opti-MEM containing 1 mM sodium pervanadate to inhibit tyrosine phosphatases. Cells were then solubilized at 4 °C in a nonionic detergent buffer (Brij lysis buffer) containing 1% Brij 96, 150 mM NaCl, 10 mM Tris-HCl, pH 7.4, 1 mM NaEDTA, 1 mM NaEGTA, 500 μ g/ml Pefabloc (Boehringer Mannheim, Mannheim, Germany), 200 μ M Na_3VO_4 , 10 mM NaF, 0.01% leupeptin, 0.11 trypsin-inhibiting units/ml aprotinin. Lysates were passed through a 22-gauge syringe and clarified by centrifugation at $10,000 \times g$ for 20 min at 4 °C. Cerebella were isolated from wild type C57Bl/6 mice (Harlan Sprague Dawley) at postnatal day 4 as described (27), and Brij extracts were prepared similarly. Protein concentrations were determined by the micro-BCA method (Pierce).

The efficiency of solubilization of $p59^{fyn}$ and $pp60^{c-src}$ was evaluated in pilot experiments with a membrane fraction from fetal rat brain using a variety of nonionic detergents including Brij 96, Triton X-100, digitonin, *N*-octylglucoside, CHAPS, and sodium deoxycholate. Only Brij 96 (0.1–1%) and to a lesser extent Triton X-100 (1%) afforded complete solubilization with retention of kinase activity, as judged by the distribution of $p59^{fyn}$ and $pp60^{c-src}$ protein and kinase activities in supernatant and pellet fractions (17).

Antibody-induced Cross-linking and Incubation with NCAM Fusion Protein

COS-7 or B35 neuroblastoma cells cultured in 100-mm tissue culture dishes were rinsed in serum-free Opti-MEM then incubated with NCAM mAb (25 μ g/ml; Chemicon 310 or NCAM 16.2) or normal rat IgG for 30 min at 4 °C. Cells were rinsed with Opti-MEM and incubated with 5 μ g/ml anti-rat or anti-mouse IgG for 20 min at 4 °C and then transferred to 37 °C. Alternatively, cells were incubated with the NCAM Fc-fusion protein (50 μ g/ml) for 30 min at 4 °C. Prior to lysis, cells were incubated for 5 min in Opti-MEM containing 1 mM sodium pervanadate at 4 °C; then extracts were prepared in Brij lysis buffer (0.75 ml). NCAM immunoprecipitates were collected by the addition of 35 μ l of a 1:1 (v/v) suspension of Protein G-Sepharose in Brij lysis buffer.

Immunoprecipitation, *In Vitro* Kinase Assays, and Immunoblotting

Immunoprecipitation—Cell lysates were precleared by incubation with normal IgG for 30 min and Protein A- or Protein G-Sepharose beads (Sigma) for 30 min followed by centrifugation at 14,000 rpm. Primary antibody in excess amount (1 μ g) or normal IgG was added to equal amounts of extract (500 μ g to 1 mg) in a 1-ml volume, and extracts were incubated with gentle inversion for 1 h at 4 °C. Immune complexes were recovered by the addition of 40 μ l of Protein A- or Protein G-Sepharose for polyclonal or monoclonal antibodies, respectively. Pellets were collected by centrifugation at $10,000 \times g$ for 1 min and washed 4 times with Brij lysis buffer.

***In Vitro* Kinase Assays**—Immunoprecipitates were incubated in a kinase reaction buffer (30 μ l) containing 7.5 μ Ci of [γ -³²P]ATP (3000 Ci/mmol), 50 mM Tris-HCl, pH 7.4, 3 mM MnCl₂, 3 mM MgCl₂, 100 mM NaCl, 100 μ M Na_3VO_4 , and 1 μ M ATP. *In vitro* kinase assays of immune complexes from cerebellum were performed with 15 μ Ci of [γ -³²P]ATP (3000 Ci/mmol) per reaction without additional unlabeled ATP. Phosphorylation was allowed to proceed for 20 min at room temperature. Beads were washed and proteins eluted by boiling for 10 min in 3% SDS, 50 mM Tris-HCl, pH 7.4, 150 mM NaCl, and 100 μ M Na_3VO_4 , with removal of beads by centrifugation. For re-immunoprecipitation, super-

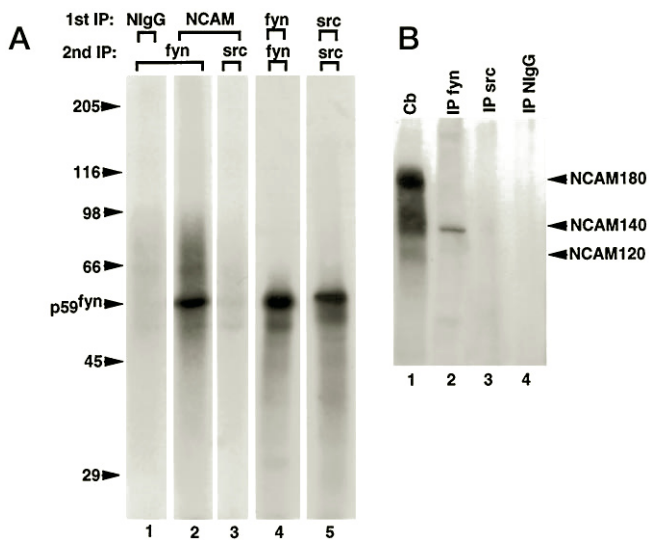


FIG. 1. Association of $p59^{fyn}$ with NCAM140 in mouse cerebellum. A, cerebellar extracts from postnatal day 4 mice (PND4) were prepared in Brij lysis buffer and subjected to immunoprecipitation (*1st IP*) with nonimmune mouse IgG or a pool of NCAM antibodies (mAb 14.2 and mAb 5B8). Immune complexes were subjected to *in vitro* kinase assays with $[\gamma\text{-}^{32}\text{P}]\text{ATP}$, solubilized in 3% SDS, diluted in Brij lysis buffer, and re-immunoprecipitated with Fyn pAb 3 or Src mAb 327 as indicated (*2nd IP*). The resulting immune complexes were separated by reducing SDS-PAGE and visualized by autoradiography for 22 h (lanes 1–3) or 1 h (lanes 4 and 5). B, mouse cerebellar extracts in Brij lysis buffer were untreated (*Cb*; 25 μg) or subjected to immunoprecipitation (1.5 mg) with Fyn pAb 3, Src mAb 327, and nonimmune IgG (lanes 2–4). The immune complexes were separated by nonreducing SDS-PAGE and subjected to immunoblotting with NCAM pAb 1505 followed by enhanced chemiluminescence.

natants were diluted 1/12 in Brij lysis buffer, incubated with antibody (1 μg) for 1 h, and Protein A- or Protein G-Sepharose for 30 min. The beads were washed 3 times, heated to 95 $^{\circ}\text{C}$ for 3 min in SDS sample buffer, and the supernatant proteins subjected to SDS-PAGE, pH 8.8. Autoradiography on Dupont Chronex 6-plus x-ray film was carried out with intensifying screens at -70°C .

Stoichiometry of Association of $p59^{fyn}$ and $p125^{fak}$ with NCAM—NCAM140 was immunoprecipitated from Brij lysis buffer extracts of mouse cerebellum or cell cultures under conditions of antibody excess, and *in vitro* kinase assays were carried out as described above and in Fig. 1A. Proteins were eluted from the immune complexes, incubated with Fyn or Fak antibodies, and separated by SDS-PAGE under reducing conditions. The amount of ^{32}P -labeled $p59^{fyn}$ or $p125^{fak}$ was quantitated by Cerenkov counting of excised gel bands and compared with the total amount of ^{32}P -labeled $p59^{fyn}$ or $p125^{fak}$ immunoprecipitated from the same amount of extract protein. In some experiments stoichiometry was estimated by densitometric scanning of bands obtained by enhanced chemiluminescence of immunoblots.

Immunoblotting—Proteins were separated under nonreducing ($p59^{fyn}$) or reducing ($p125^{fak}$) conditions by SDS-PAGE, pH 8.8, and transferred to nitrocellulose filters (Schleicher & Schuell). Filters were blocked for 2 h in 2% bovine serum albumin and incubated overnight with primary antibodies. After 5 washes of 5 min each in TBS/Tween buffer (0.02 M Tris-HCl, pH 7.4, 150 mM NaCl, 0.05% Tween 20), filters were incubated with a 1:10,000 dilution of goat anti-rabbit secondary antibody conjugated to horseradish peroxidase (Sigma) for 1 h at room temperature, followed by 5 washes in TBS/Tween buffer. Proteins were visualized by enhanced chemiluminescence (Amersham Corp.). To reprobe immunoblots the membranes were stripped for 30 min at 50 $^{\circ}\text{C}$ in 10% SDS, 0.02 M Tris, pH 6.8, 100 mM β -mercaptoethanol, and rinsed with TBS/Tween.

RESULTS

$p59^{fyn}$ Associates with the NCAM140 Isoform in Mouse Cerebellum—At postnatal day 4 (PND4) the mouse cerebellum contains many developing neurons engaged in migration and axonal growth, and it expresses $p59^{fyn}$, $pp60^{c-src}$ (27), and the three major NCAM isoforms (NCAM180, -140, and -120) (Fig. 1). To investigate a potential physical association between

$p59^{fyn}$ and NCAM in the developing cerebellum, NCAM and associated proteins were immunoprecipitated from extracts of PND4 mouse cerebellum prepared in nonionic Brij 96 detergent-containing buffer (Brij lysis buffer) using a pool of two NCAM monoclonal antibodies recognizing all three NCAM isoforms. The resulting immunoprecipitates were subjected to *in vitro* kinase assays with $[\gamma\text{-}^{32}\text{P}]\text{ATP}$ to label active tyrosine kinases present in the NCAM complexes by autophosphorylation. This method was used because it afforded greater sensitivity and quantitation than immunoblotting. Immune complexes were solubilized in 3% SDS, diluted 1/12 in Brij lysis buffer, and re-immunoprecipitated with Fyn or Src antibodies. $p59^{fyn}$ was found to co-immunoprecipitate with NCAM from the mouse cerebellar extracts, whereas $pp60^{c-src}$ did not significantly co-immunoprecipitate with NCAM (Fig. 1A). $p59^{fyn}$ and $pp60^{c-src}$ kinase activities were expressed at approximately equal levels in the PND4 mouse cerebellum (Fig. 1A), indicating a selective association of NCAM with $p59^{fyn}$, which was in accord with the neurite outgrowth properties of *fyn*- and *src*-minus neurons (27).

The specificity of association between NCAM and $p59^{fyn}$ was ascertained by a reverse immunoprecipitation protocol in which $p59^{fyn}$ or $pp60^{c-src}$ was first immunoprecipitated from mouse cerebellar extracts (PND4), and the resulting complexes were assayed for the presence of NCAM by immunoblotting with an NCAM polyclonal antibody recognizing all three isoforms. This approach also revealed the particular isoform(s) of NCAM co-immunoprecipitating with $p59^{fyn}$. Mouse cerebellum expressed equivalent amounts of NCAM180 and NCAM140 and a small amount of NCAM120 at this stage in development (Fig. 1B). The broad bands were most likely due to polysialylation of NCAM isoforms. However, only the NCAM140 isoform co-immunoprecipitated with $p59^{fyn}$ (Fig. 1B). The sharpening of the NCAM140 band probably resulted from desialylation during heat treatment in SDS. Neither the NCAM180 transmembrane isoform nor the GPI-linked NCAM120 isoform were present to a significant degree in the $p59^{fyn}$ immune complexes. In addition, none of the NCAM isoforms co-immunoprecipitated with $pp60^{c-src}$.

By comparing the amount of ^{32}P -labeled $p59^{fyn}$ in the NCAM immunoprecipitates to the total amount of ^{32}P -labeled $p59^{fyn}$ in immunoprecipitates from an equivalent amount of mouse cerebellar extract, it was estimated that 1% of the $p59^{fyn}$ molecules in the PND4 mouse cerebellum associated with NCAM140. Conversely, by comparing the amount of NCAM140 in $p59^{fyn}$ immunoprecipitates to total NCAM140 immunoprecipitated from mouse cerebellar extracts by densitometric scanning (Fig. 1B), it was estimated that approximately 3% of the NCAM140 in mouse cerebellum was associated with $p59^{fyn}$. This stoichiometry approximated that of $p59^{fyn}$ associated with the T cell receptor ζ subunit (1–5%) (41), myelin-associated glycoprotein (5%) (33), and B cell receptor protein Ig- δ (3–7%) (42), and was suggestive of a low affinity interaction. However, the actual stoichiometry could be higher, since some complexes might dissociate during lysis.

$p59^{fyn}$ Interacts with NCAM140 and a 125-kDa Phosphoprotein in Transfected Cells—Cell lines expressing transfected NCAM or *fyn* cDNAs were used to further investigate the specificity of association of $p59^{fyn}$ with NCAM isoforms. Simian COS-7 cells were cotransfected for transient expression with pcDNA3 plasmids containing cDNAs encoding NCAM140 or NCAM180 (each lacking the VASE sequence), together with plasmids encoding brain-enriched forms of $p59^{fyn}$ (B form) or $pp60^{c-src}$ (*src*⁺ isoform with a 6-amino acid insert). Pilot enzyme-linked immunosorbent assay results showed that COS-7 cells expressed very low levels of endogenous $p59^{fyn}$ and

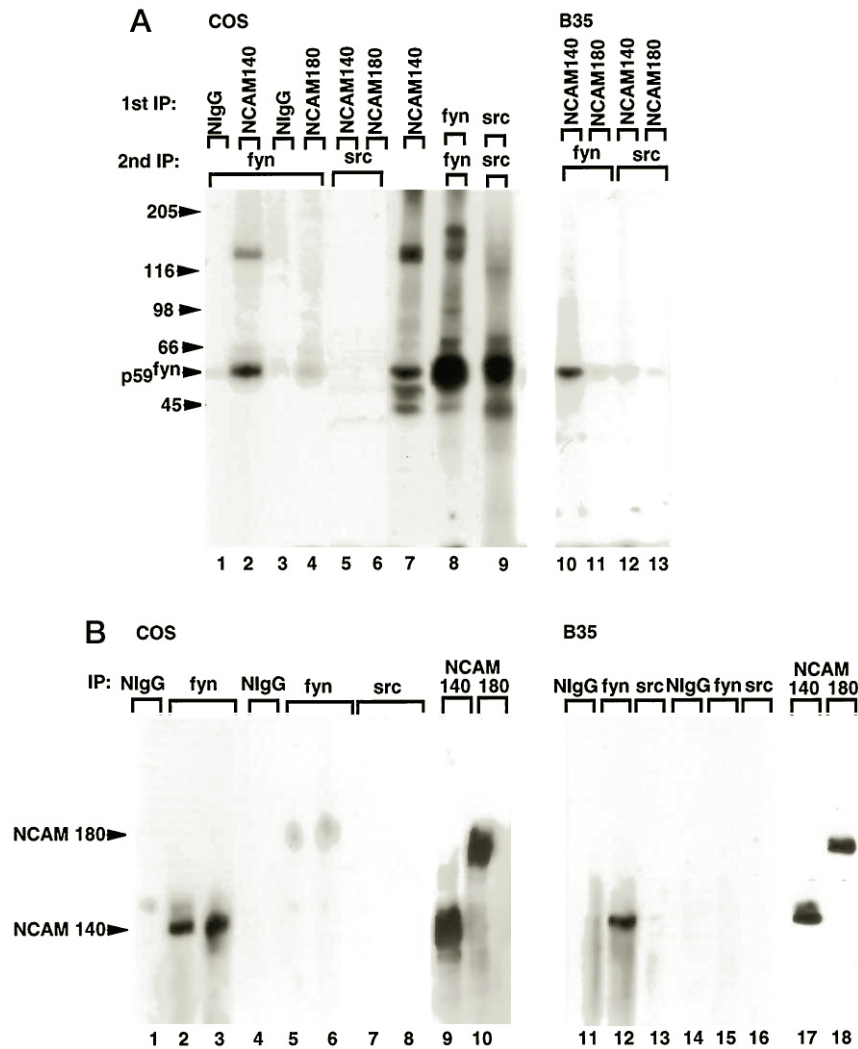


FIG. 2. Association of p59^{fyn} with NCAM 140 in transfected COS-7 and rat B35 neuroblastoma cells. *A*, COS-7 cells were cotransfected for transient expression of the following cDNAs: NCAM140 and *fyn* (lanes 1, 2, 7, and 8), NCAM180 and *fyn* (lanes 3 and 4), NCAM140 and *src* (lanes 5 and 9), NCAM180 and *src* (6). Rat B35 neuroblastoma cell lines stably expressing NCAM isoforms were transfected for transient expression of *fyn* or *src* cDNAs as indicated (lanes 10–13). Proteins were immunoprecipitated from extracts (500 μ g) prepared in Brij lysis buffer using a pool of NCAM mAb antibodies (14.2, 5B8), nonimmune IgG, Fyn 3 pAb, or Src mAb 327 (1st IP). Immune complexes were subjected to *in vitro* kinase assays with [γ -³²P]ATP, solubilized in 3% SDS, diluted in Brij lysis buffer, and re-immunoprecipitated using Fyn or Src antibodies (2nd IP). The resulting immune complexes were separated by reducing SDS-PAGE and visualized by autoradiography for 1 h (lanes 7–9), 10 h (lanes 1–6), or 24 h (lanes 10–13). *B*, COS-7 cells were transfected for transient expression of the following cDNAs: NCAM140 and *fyn* (lanes 1, 2, and 9), NCAM140 (with VASE) and *fyn* (lane 3), NCAM180 and *fyn* (lanes 4, 5, and 10), NCAM180 (with VASE) and *fyn* (lane 6), NCAM140 and *src* (lane 7), NCAM180 and *src* (lane 8). Rat B35 neuroblastoma cell lines stably expressing the following NCAM isoforms were transfected for transient expression of *fyn* or *src* cDNAs: NCAM140 and *fyn* (lanes 11, 12, and 17), NCAM140 and *src* (lane 13), NCAM180 and *fyn* (lanes 14, 15, and 18), NCAM180 and *src* (lane 16). Proteins were immunoprecipitated from extracts (750 μ g) prepared in Brij lysis buffer using nonimmune IgG, Fyn pAb 3, Src mAb 327, or the pool of NCAM antibodies (mAb 14.2, 5B8) as indicated (IP). Immune complexes were subjected to nonreducing SDS-PAGE followed by immunoblotting with NCAM pAb 1505 using enhanced chemiluminescence.

pp60^{c-src}, which did not contribute significantly to the high levels expressed from transfected cDNAs. NCAM was immunoprecipitated from Brij lysates of transfected COS-7 cells 48 h after transfection, and immune complexes were subjected to *in vitro* kinase reactions with [γ -³²P]ATP. Proteins in the immune complexes were solubilized in 3% SDS, diluted 1/12 in Brij lysis buffer, and re-immunoprecipitated with Fyn or Src antibodies. This experiment showed that the B isoform of p59^{fyn} associated strongly with NCAM140 (without VASE) and to a much lesser degree with NCAM180 (Fig. 2A). Conversely, pp60^{c-src} was not associated with either NCAM140 or NCAM180 (Fig. 2A). The alternative form of pp60^{c-src} lacking the insert in the SH3 domain also failed to associate with NCAM140 or NCAM180 when transiently expressed in COS-7 cells (not shown). An endogenous protein of approximately 125 kDa was phosphorylated in the NCAM140 immune complexes, along with a 59-kDa

protein which most likely represented p59^{fyn}, and several proteins in the 45–55-kDa range (Fig. 2A, lane 7). Notably, the 125-kDa phosphoprotein persisted in the Fyn re-immunoprecipitates after solubilization of the immune complexes in SDS and dilution in Brij lysis buffer (lane 2). This most likely resulted from reassociation after dilution of the detergent and a further incubation for 1 h at 4 °C. The 125-kDa protein was not present in either the Fyn re-immunoprecipitates from NCAM180 immune complexes (lane 4) or the Src re-immunoprecipitates from immune complexes containing either NCAM isoform (lanes 5 and 6). In the reverse immunoprecipitation, p59^{fyn} was first immunoprecipitated from the transfected COS-7 cells followed by NCAM immunoblotting (Fig. 2B). These results confirmed that NCAM140 and little NCAM180 co-immunoprecipitated with p59^{fyn}, whereas neither isoform of NCAM co-immunoprecipitated with pp60^{c-src}.

To investigate the $p59^{fyn}$ association in a neuronal cell type known to express moderate levels of NCAM isoforms on the cell surface, the central nervous system-derived rat B35 neuroblastoma cell line was used for similar co-immunoprecipitation experiments. Differentiated B35 neuroblastoma cells exhibit neuronal properties including membrane excitability and expression of enzymes involved in neurotransmitter metabolism (43). Stably transformed B35 cell lines have been developed that express NCAM140 or NCAM180 (each with and without VASE) at equivalent levels on their cell surface (9) (Fig. 2B, lanes 17 and 18). Because the cells express much lower levels of $p59^{fyn}$ and $pp60^{c-src}$ as detected by immunoprecipitation (not shown), the B35 cell lines were transiently transfected with *fyn* (B form) or *src* (*c-src*⁺) pcDNA3 plasmids and assayed 48 h later for association with NCAM. NCAM was immunoprecipitated from Brij lysates of transfected B35 neuroblastoma cells and immune complexes subjected to *in vitro* phosphorylation with $[\gamma\text{-}^{32}\text{P}]\text{ATP}$. Immune complexes were solubilized and re-immunoprecipitated with Fyn or Src antibodies. $p59^{fyn}$ was found to co-immunoprecipitate with NCAM140 and not NCAM180 (each without VASE), whereas $pp60^{c-src}$ did not co-immunoprecipitate with either NCAM isoform (Fig. 2A). The reverse immunoprecipitation confirmed these results (Fig. 2B).

Cerenkov counting of excised $p59^{fyn}$ bands revealed that 3% of the total $p59^{fyn}$ immunoprecipitated from COS-7 cells under conditions of antibody excess preferentially bound to NCAM140, whereas densitometric scanning of NCAM immunoblots indicated that 5% of the total NCAM140 immunoprecipitated from COS-7 cells bound to $p59^{fyn}$. Equivalent levels of NCAM140 and -180 were expressed in the transfected COS-7 cells as shown by immunoblotting (Fig. 2B, lanes 9 and 10). Immunoperoxidase staining of formaldehyde-fixed cell cultures showed pronounced staining of NCAM140 and NCAM180 on the cell surface (not shown). Similarly, comparable levels of $p59^{fyn}$ and $pp60^{c-src}$ kinase activity were expressed in the transfected COS-7 cells (lanes 8 and 9).

A large portion of NCAM in the adult brain contains the alternatively spliced VASE exon in the fourth Ig domain, a modification that down-regulates neurite outgrowth (8–10). The presence of the VASE exon in NCAM140 or NCAM180 did not alter the association of $p59^{fyn}$ in transfected COS-7 cells (Fig. 2B, lanes 3 and 6) indicating that the neurite growth inhibitory effect of the VASE isoform was not due to $p59^{fyn}$ dissociation from the NCAM complex.

$p59^{fyn}$ has been reported to associate with the GPI-linked proteins F3/F11/contactin (44), Thy-1 (45), decay accelerating factor, or CD59 (46), but these associations can be disrupted in *N*-octylglucoside, a nonionic detergent resembling glycolipids (44, 45). The association of $p59^{fyn}$ with NCAM140 was stable in cell extracts prepared with *N*-octylglucoside (1%) or other nonionic detergents CHAPS and Triton X-100 (1%). Stability in 1% *N*-octylglucoside indicated that the $p59^{fyn}$ -NCAM140 association was not likely to be mediated by a GPI-linked molecule. Moreover, $p59^{fyn}$ did not co-immunoprecipitate with the GPI-linked NCAM120 isoform from mouse cerebellum (Fig. 1).

Identification of the $p59^{fyn}$ -associated Protein as $p125^{fak}$ —Because $p59^{fyn}$ was known to associate with the focal adhesion kinase $p125^{fak}$ in nonneuronal cells (47), it was logical to investigate whether the 125-kDa protein that was phosphorylated in the NCAM140- $p59^{fyn}$ immune complexes from COS-7 cells was $p125^{fak}$. To this end NCAM140 was immunoprecipitated from Brij extracts of COS-7 cells transiently expressing NCAM140 and *fyn* cDNAs. The resulting NCAM immune complexes were subjected to *in vitro* kinase assays with $[\gamma\text{-}^{32}\text{P}]\text{ATP}$, solubilized, and re-immunoprecipitated with Fak antibodies. A ^{32}P -labeled 125-kDa protein specifically immuno-

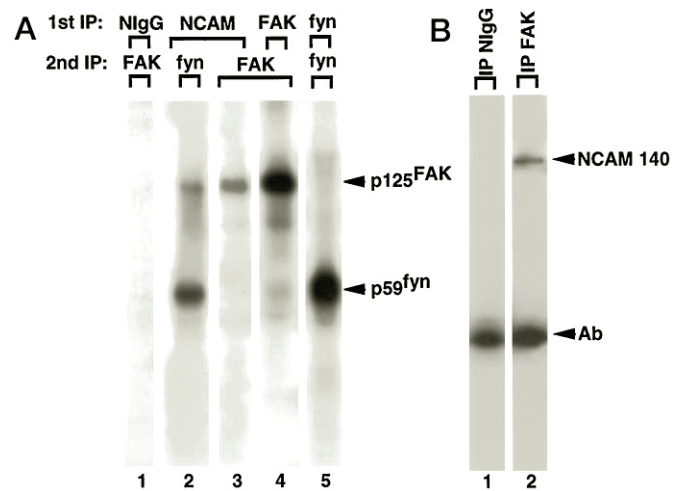


Fig. 3. $p125^{fak}$ associates with NCAM140 in COS-7 cells. A, COS-7 cells transiently expressing NCAM140 and *fyn* cDNAs were lysed in Brij lysis buffer and immunoprecipitated (1st IP) with normal IgG, a pool of NCAM antibodies (mAb 14.2, 5B8), Fak polyclonal antibody BC3, or Fyn pAb 3. Immune complexes were subjected to *in vitro* kinase assays with $[\gamma\text{-}^{32}\text{P}]\text{ATP}$ and re-immunoprecipitated with Fak or Fyn antibodies (2nd IP). The resulting immune complexes were resolved by reducing SDS-PAGE and visualized by autoradiography for 22 h (lanes 1–3) or for 7 h (lanes 4 and 5). B, COS-7 cell lines transiently expressing NCAM140 and *fyn* cDNAs were lysed in Brij lysis buffer and immunoprecipitated with normal IgG or Fak pAb BC3. Complexes were resolved by reducing SDS-PAGE and visualized by immunoblotting with NCAM pAb 1505 using enhanced chemiluminescence. The position of antibody heavy chain recognized by the secondary antibodies (Ab).

precipitated with Fak antibodies (Fig. 3A, lane 3). This protein was also evident in re-immunoprecipitations with Fyn antibodies (Fig. 2A, lane 2; Fig. 3A, lane 2). $p59^{fyn}$ was not evident in the Fak re-immunoprecipitations (Fig. 3A, lane 3) possibly due to steric hindrance of $p59^{fyn}$ by the Fak antibody. COS-7 cells expressed high levels of endogenous $p125^{fak}$ (Fig. 3A, lane 4), which approximated the levels of $p59^{fyn}$ transiently expressed from the transfected *fyn* plasmid (lane 5). As shown in Fig. 2A, $p125^{fak}$ did not co-immunoprecipitate with NCAM180 or with $pp60^{c-src}$ from COS-7 cells expressing either NCAM180 or NCAM140. In the reverse immunoprecipitation protocol, $p125^{fak}$ was immunoprecipitated from Brij extracts of COS-7 cells transiently expressing NCAM140 and *fyn* cDNAs, and the immune complexes were subjected to immunoblotting with NCAM antibodies (Fig. 3B). NCAM140 was found to specifically co-immunoprecipitate with $p125^{fak}$.

To estimate the stoichiometry of the association, the amount of ^{32}P -labeled $p125^{fak}$ re-immunoprecipitated from solubilized NCAM140 immune complexes was compared with the total amount of ^{32}P -labeled $p125^{fak}$ immunoprecipitated from an equal amount of COS-7 cell extract. Approximately 1% of the $p125^{fak}$ expressed in COS-7 cells was present in NCAM140 immune complexes. In the reverse immunoprecipitation, densitometric scanning indicated that approximately 3% of the NCAM140 expressed in COS-7 cells associated with $p125^{fak}$, a stoichiometry of similar magnitude to that of the NCAM140- $p59^{fyn}$ association. A 125-kDa protein in association with the NCAM140- $p59^{fyn}$ complex was not detected by co-immunoprecipitation from mouse cerebellar extracts (Fig. 1). This may be due to lower expression of $p125^{fak}$ in the cerebellum at PND4 or less recruitment of $p125^{fak}$ to NCAM complexes at this stage.

NCAM Binding Induces the Phosphorylation and Recruitment of $p125^{fak}$ —To examine the functional interaction between $p125^{fak}$ and NCAM, tyrosine phosphorylation of $p125^{fak}$ was assayed following antibody-induced cross-linking of NCAM140. COS-7 cells transiently expressing NCAM140 and

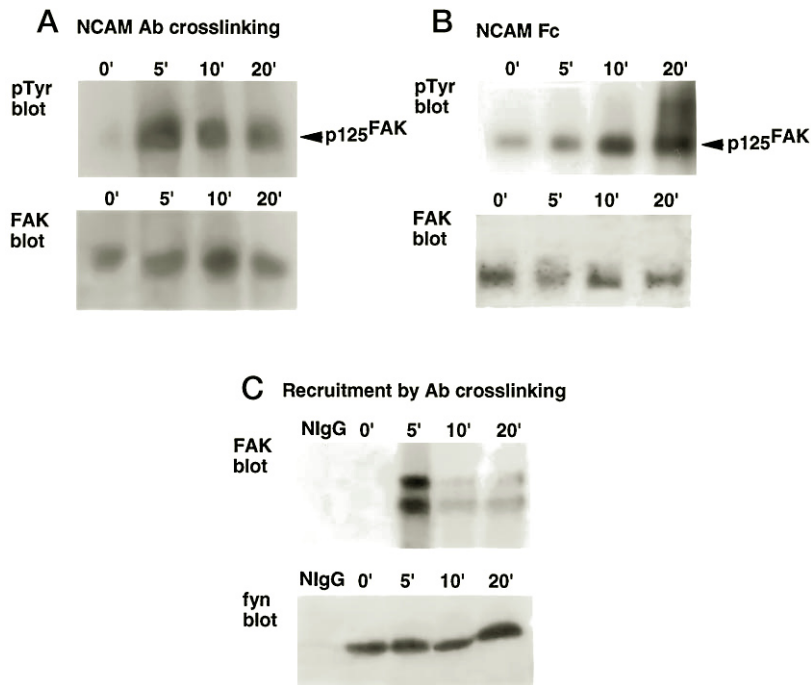


FIG. 4. **Stimulation of NCAM140 in COS-7 cells increases $p125^{fak}$ tyrosine phosphorylation and recruitment.** *A*, COS-7 cells transiently expressing NCAM140 and $p59^{fyn}$ were incubated with NCAM mAb 16.2 (25 $\mu\text{g}/\text{ml}$), followed by anti-mouse IgG. At 0, 5, 10, and 20 min, cells were lysed in Brij lysis buffer, and $p125^{fak}$ was immunoprecipitated from extracts (500 μg) with Fak pAb HUB3 and subjected to reducing SDS-PAGE. $p125^{fak}$ was analyzed by immunoblotting with phosphotyrosine mAb 4G10 using enhanced chemiluminescence. The same filter was stripped and reblotted with Fak pAb HUB3. Similar results were obtained with NCAM mAb 310. *B*, COS-7 cells were incubated with soluble NCAM-Fc fusion protein (50 $\mu\text{g}/\text{ml}$) for 0, 5, 10, and 20 min and $p125^{fak}$ immunoprecipitated with Fak pAb HUB3 followed by immunoblotting with phosphotyrosine mAb 4G10. The same filter was stripped and reblotted with Fak pAb HUB3. *C*, COS-7 cells transiently expressing NCAM140 and $p59^{fyn}$ were incubated with normal mouse IgG and anti-mouse IgG for 5 min (NlgG) or NCAM mAb 16.2 and anti-mouse IgG for 0, 5, 10, and 20 min. NCAM immune complexes and associated proteins were collected by precipitation with Protein-G Sepharose from Brij extracts. Complexes were resolved on nonreducing SDS-PAGE and analyzed for $p125^{fak}$ or $p59^{fyn}$ by immunoblotting with Fak pAb HUB3 or Fyn pAb 3. Recruitment experiments were repeated three ($p125^{fak}$) and four times ($p59^{fyn}$) with the same results.

$p59^{fyn}$ were incubated for 30 min at 4 °C with an NCAM monoclonal antibody (mAb 16.2) directed against an extracellular epitope in the homophilic binding site of NCAM under conditions that allowed antibody binding but prevented internalization (48). Secondary antibodies were then added and cells transferred to 37 °C to cross-link NCAM molecules on the cell surface. At various times after treatment cells were lysed in Brij lysis buffer and $p125^{fak}$ was immunoprecipitated with Fak antibodies. Immunoblotting was carried out with phosphotyrosine antibodies and then the blot was stripped and reprobed with Fak antibodies. This experiment revealed an increase in the tyrosine phosphorylation of $p125^{fak}$ without a significant change in $p125^{fak}$ protein (Fig. 4). Maximum phosphorylation was observed 5 min following NCAM antibody treatment and then diminished, possibly due to the action of tyrosine phosphatase activity in cells. Omission of secondary antibodies did not stimulate tyrosine phosphorylation of $p125^{fak}$ (not shown). By densitometric scanning it was estimated that total $p125^{fak}$ tyrosine phosphorylation was stimulated approximately 50-fold following NCAM antibody ligation. To address whether these changes were also induced by NCAM protein, COS-7 cells were treated with a soluble NCAM fusion protein in which the NCAM extracellular region was fused to the Fc portion of human Ig (NCAM-Fc). Immunoprecipitation of $p125^{fak}$ followed by immunoblotting with phosphotyrosine or Fak antibodies revealed an increase in specific $p125^{fak}$ tyrosine phosphorylation (Fig. 4). However, $p125^{fak}$ phosphorylation induced by NCAM-Fc was somewhat slower and less pronounced than antibody-induced ligation of NCAM.

To address whether $p125^{fak}$ was recruited to NCAM complexes, COS-7 cells transiently expressing NCAM140 and $p59^{fyn}$ were treated with nonimmune IgG or NCAM monoclonal

antibodies followed by secondary antibodies. Cells were lysed and immune complexes containing NCAM were collected by precipitation with Protein G-Sepharose. Immunoblotting with Fak antibodies showed that $p125^{fak}$ was strongly recruited into NCAM complexes within 5 min of stimulation (Fig. 4). Basal levels of $p125^{fak}$ complexed to NCAM at $t = 0$ were not evident by immunoblotting with Fak antibodies, although they were evident by the more sensitive *in vitro* phosphorylation assay (Figs. 2 and 3). $p125^{fak}$ appeared to dissociate from the NCAM complexes during antibody-induced ligation of NCAM in COS-7 cells, and this occurred concomitant with the observed dephosphorylation of $p125^{fak}$ shown above. This may indicate that $p125^{fak}$ recruitment to the NCAM complex was dependent on $p125^{fak}$ tyrosine phosphorylation. The $p125^{fak}$ doublet observed in the recruitment experiment was not reproducibly seen, but often the band appeared broad. A similar Fak doublet has been previously reported (49) and may be a consequence of differential phosphorylation (50, 51) or proteolytic degradation. The possibility of cross-reactivity of the Fak antibodies with a Fak-related kinase cannot be ruled out, but preliminary experiments with antibodies against PYK2/CADTK/CAK β (52) (from S. Earp, University of North Carolina) did not show NCAM antibody-induced tyrosine phosphorylation of this kinase.

Unlike $p125^{fak}$, $p59^{fyn}$ was not recruited to the NCAM complexes upon antibody-induced ligation of NCAM140 in COS-7 cells under the same conditions but instead appeared to be constitutively bound to NCAM140. NCAM complexes isolated at various times after antibody treatment of cells were subjected to immunoblotting with Fyn antibodies and showed levels of $p59^{fyn}$ protein in NCAM complexes that remained more or less unchanged during the 20 min of antibody treatment (Fig. 4).

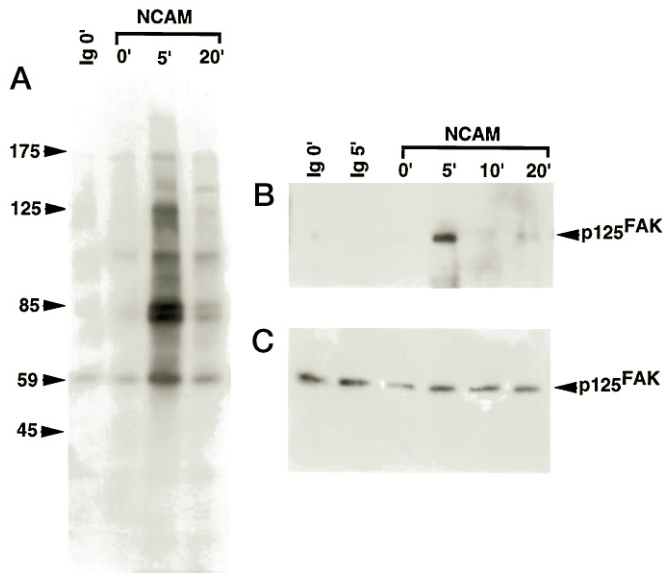


FIG. 5. Stimulation of NCAM140 in B35 neuroblastoma cells increases $p125^{fak}$ tyrosine phosphorylation. Rat B35 neuroblastoma cells stably expressing NCAM140 and transiently expressing $p59^{fyn}$ were incubated with nonimmune mouse IgG or mouse NCAM mAb 16.2 followed by anti-mouse IgG for 0, 5, 10, and 20 min. *A*, cell extracts prepared in Brij lysis buffer (25 μ g) were subjected to SDS-PAGE and immunoblotting with phosphotyrosine mAb 4G10. Control samples (*Ig* 0', *Ig* 5') were incubated with nonimmune mouse IgG and anti-mouse IgG for 0 and 5 min. *C*, the same nitrocellulose filter in *B* was stripped and reblotted with Fak pAb HUB3.

The 125-kDa phosphoprotein identified as $p125^{fak}$ in NCAM140 immune complexes from COS-7 cells was not evident in NCAM140 immunoprecipitates from unstimulated B35 neuroblastoma cells (Fig. 3). This may have been due to lower levels of $p125^{fak}$ and to fewer cell-cell contacts in B35 cultures, which would reduce the basal levels of $p125^{fak}$ recruited to NCAM. However, NCAM-induced tyrosine phosphorylation of total immunoprecipitated $p125^{fak}$ could be measured. Accordingly, B35 cells expressing NCAM140 and $p59^{fyn}$ were treated with primary NCAM antibodies and secondary antibodies, and then tyrosine phosphorylation of total cell proteins and $p125^{fak}$ was examined by immunoblotting with phosphotyrosine antibodies (Fig. 5A). Transient tyrosine phosphorylation was observed in several proteins, including those of 125, 110, 85 (doublet), and 59 kDa within 5 min of antibody treatment (Fig. 5A). Immunoprecipitation with Fak antibodies followed by immunoblotting with phosphotyrosine antibodies identified the 125-kDa protein as $p125^{fak}$ and demonstrated that $p125^{fak}$ was rapidly (within 5 min) and transiently tyrosine-phosphorylated upon antibody-mediated NCAM ligation (Fig. 5B). The amount of $p125^{fak}$ protein was unchanged as shown by immunoblotting with Fak antibodies (Fig. 5C). The relative increase in $p125^{fak}$ tyrosine phosphorylation could not be calculated because basal levels of phosphotyrosine-modified $p125^{fak}$ were undetectable. Furthermore, $p125^{fak}$ was not detectable in NCAM immune complexes from B35 cell extracts by immunoblotting with Fak antibodies after antibody-induced ligation of NCAM. Because 1–3% of the $p125^{fak}$ expressed in B35 cells would not be detectable, $p125^{fak}$ could be recruited to NCAM complexes with a stoichiometry similar to that occurring in COS-7 cells.

NCAM Binding Activates Tyrosine Phosphorylation of $p59^{fyn}$ —Treatment of B35 cells expressing NCAM140 and $p59^{fyn}$ with primary NCAM antibodies followed by secondary

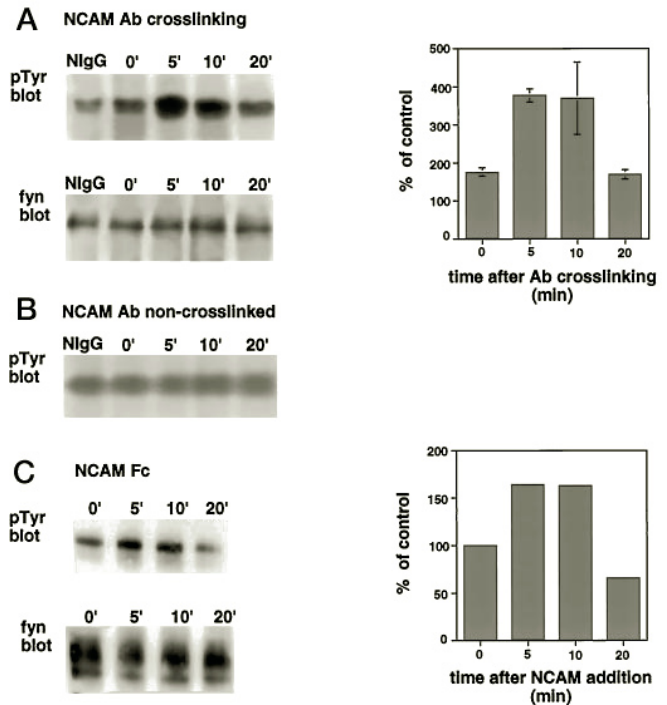


FIG. 6. Stimulation of NCAM140 in B35 neuroblastoma cells increases tyrosine phosphorylation of $p59^{fyn}$. *A*, B35 neuroblastoma cells stably expressing NCAM140 and transiently expressing $p59^{fyn}$ were incubated with nonimmune rat IgG or rat NCAM mAb 310 followed by anti-rat IgG. At 0 min (*NlgG*) or 0, 5, 10, and 20 min (*NCAM Ab*) after addition of secondary antibody, cells were lysed in Brij lysis buffer, and $p59^{fyn}$ was immunoprecipitated from each extract (500 μ g) with Fyn pAb 3. Immune complexes were resolved on nonreducing SDS-PAGE and analyzed for $p59^{fyn}$ tyrosine phosphorylation by immunoblotting with phosphotyrosine mAb 4G10. The same filter was stripped and reblotted for $p59^{fyn}$ protein with Fyn pAb 3. Densitometric quantification of $p59^{fyn}$ tyrosine phosphorylation from four cross-linking experiments is shown at the right and expressed as % of NlgG control. *Bars* indicate standard errors. *B*, B35 neuroblastoma cells expressing NCAM140 and $p59^{fyn}$ were incubated with nonimmune IgG for 0 min or NCAM mAb 310 for 0, 5, 10, and 20 min. Extracts were prepared in Brij lysis buffer and immunoprecipitated (500 μ g) with Fyn pAb 3. Immune complexes were resolved on nonreducing SDS-PAGE and analyzed for $p59^{fyn}$ tyrosine phosphorylation by immunoblotting with phosphotyrosine mAb 4G10. *C*, B35 neuroblastoma cells expressing NCAM140 and $p59^{fyn}$ were incubated with soluble NCAM-Fc protein (50 μ g/ml) for 0, 5, 10, and 20 min, and $p59^{fyn}$ was immunoprecipitated with Fyn pAb 3 from Brij extracts, followed by immunoblotting with phosphotyrosine mAb 4G10. The same filter was stripped and reblotted with Fyn pAb 3. Densitometric quantification of $p59^{fyn}$ tyrosine phosphorylation is expressed at the right as % of 0 min control. (This experiment was repeated with similar kinetics and extent of $p59^{fyn}$ activation under slightly different conditions in which NCAM-Fc was added to cells at 4 $^{\circ}$ C and then returned to 37 $^{\circ}$ C.)

antibodies caused a rapid and transient tyrosine phosphorylation of $p59^{fyn}$ (Fig. 6A). Immunoprecipitation with Fyn antibodies followed by phosphotyrosine immunoblotting revealed maximal activation of $p59^{fyn}$ tyrosine phosphorylation (approximately 4-fold) at 5–10 min after cross-linking. The amount of $p59^{fyn}$ protein was unchanged as shown by immunoblotting with Fyn antibodies (Fig. 6A). Treatment of cells with two different NCAM antibodies (mAb 16.2 and mAb 310) elicited the same extent and kinetics of phosphorylation. $p59^{fyn}$ tyrosine phosphorylation was of similar magnitude to that induced by antibody-mediated ligation of myelin-associated glycoprotein (33). Clustering of NCAM on the cell surface appeared to be necessary for maximal $p59^{fyn}$ phosphorylation, since phosphotyrosine levels of $p59^{fyn}$ were unchanged in cells treated with primary NCAM antibodies alone (Fig. 6B, non-

crosslinked). Triggering of B35 cells with the soluble NCAM-Fc fusion protein also resulted in a transient elevation in p59^{fy_n} tyrosine phosphorylation with maximum phosphorylation at 5–10 min and then declining (Fig. 6C); however, the extent of phosphorylation was not so great as with antibody-mediated cross-linking possibly due to a lower state of oligomerization. The presence of the VASE exon in the NCAM140 isoform did not alter the extent or kinetics of p59^{fy_n} phosphorylation upon NCAM antibody treatment of B35 neuroblastoma cells stably expressing this isoform (not shown). One explanation for the smaller increase in tyrosine phosphorylation of p59^{fy_n} compared with p125^{fa_k} is that p59^{fy_n} may be initially phosphorylated to some degree on its terminal tyrosine residue (Tyr-531). This residue is known to be phosphorylated by the tyrosine kinase Csk, which negatively regulates p59^{fy_n} activity (53). Although peptide mapping studies have not been performed, NCAM binding interactions may induce dephosphorylation of Tyr-531 of p59^{fy_n} by activating a tyrosine phosphatase, followed by activation of autophosphorylation (Tyr-420).

DISCUSSION

The results reported here demonstrate a physical and functional interaction of the 140-kDa isoform of the neural cell adhesion molecule NCAM with the focal adhesion tyrosine kinase p125^{fa_k} and the *src*-related tyrosine kinase p59^{fy_n}. Antibody-mediated ligation of cell surface NCAM140 or stimulation with soluble NCAM fusion protein led to a transient increase in tyrosine phosphorylation of both p125^{fa_k} and p59^{fy_n}, suggesting that activation of these nonreceptor tyrosine kinases is a proximal event in the NCAM signal transduction pathway.

The interaction of p59^{fy_n} with NCAM was consistent with the impaired NCAM-dependent neurite growth displayed by *fy_n*-minus neurons in culture and the widespread distribution of p59^{fy_n} in developing axonal tracts and nerve growth cones (31). The binding preference of NCAM for p59^{fy_n} and not pp60^{c-*src*} was in accord with the impaired NCAM-dependent neurite outgrowth of *fy_n*-minus but not *src*-minus neurons (27). The distinct but overlapping molecular associations mediated by the SH2 and SH3 domains of *src* family members provides a molecular basis for substratum-specific cellular responses displayed by growth cones (79). Neurons display different growth cone morphologies when plated on NCAM, L1, N-cadherin, laminin, and p84 suggesting that adhesive contacts and cytoskeletal structure are differentially modulated on these substrates (54–56). A molecular basis for these differences is not easily explained by a model in which a single tyrosine kinase, the fibroblast growth factor receptor, is responsible for neurite outgrowth on NCAM, L1, and N-cadherin (57). Unlike p59^{fy_n}, we have not been able to detect tyrosine phosphorylation of the fibroblast growth factor receptor upon NCAM antibody binding in our assays. However, the fibroblast growth factor receptor may provide trophic support that is permissive for neurite extension in certain neuronal cell types.

Strict specificity was displayed by p59^{fy_n} and p125^{fa_k} for the NCAM140 transmembrane isoform. Since NCAM140 is preferentially found in free migratory growth cones in contrast to NCAM180, which is associated with stable cell contacts (3, 4), these kinases may be necessary for migration of growth cones toward their targets. A developmentally regulated isoform switch from NCAM140 to NCAM180 in neurons could facilitate the transition from growth cone to synapse by terminating p59^{fy_n} and p59^{fa_k} signaling, and down-regulation of expression of p59^{fy_n} and p59^{fa_k} during maturation (31, 58) could contribute to such a transition. A primary role for p59^{fy_n} compared with pp60^{c-*src*} in p125^{fa_k} activation is also indicated by reduced p125^{fa_k} tyrosine phosphorylation in the brains of *fy_n*-minus but

not *src*-minus mice (59), and preferential complex formation between p125^{fa_k} and p59^{fy_n} in nontransformed, nonneural cells (47).

p59^{fy_n} appeared to be constitutively bound to NCAM140, either directly or indirectly, whereas p125^{fa_k} was recruited to the NCAM complex. The binding site for p59^{fy_n} (or an adaptor protein) may reside within the cytoplasmic domain of NCAM140, because the 261-amino acid insert in the corresponding region of NCAM180 effectively disrupts the association. The NCAM140 “tail” does not contain any known phosphorylated tyrosine residues for the binding of the p59^{fy_n} SH2 domain (60, 61) or polyproline motifs for the binding of an SH3 domain (62), and hence the interaction is unlike that of p59^{fy_n} with myelin-associated glycoprotein, which is mediated by the p59^{fy_n} SH2 and SH3 domains (33). Instead, NCAM140 might interact with the amino-terminal unique domain of p59^{fy_n}, which is the most divergent region among *src* family kinases and is responsible for low affinity interactions of p59^{fy_n} with the T cell receptor ζ , CD3 ϵ , and CD3 γ subunits (41), and the B cell receptor Ig- α subunit (42). However, the tail of NCAM140 lacks an immunoreceptor tyrosine-based activation motif, which mediates the association of p59^{fy_n} with the Ig- α subunit (42) and is present in each of these receptors. Differences in polysialylation within the extracellular region of NCAM140 and -180 might also influence p59^{fy_n} binding by altering the conformation of the cytoplasmic tail or modulating the *cis* interaction of NCAM with a possible transmembrane coreceptor. Polysialylation of NCAM has been shown to be important for tangential migration of olfactory bulb interneurons (63), and its removal mimics the phenotype of NCAM-minus mice (64). Mice with gene knockouts for NCAM180 or total NCAM display similar phenotypes, suggesting that a putative function of NCAM140 (and p59^{fy_n}) in axonal growth or guidance may be partially compensated by other adhesion signaling pathways.

A possible mechanism for NCAM signaling based on the results presented here is that NCAM140 binding interactions in the membrane induce autophosphorylation of constitutively associated p59^{fy_n}, possibly through activation of a tyrosine phosphatase that dephosphorylates p59^{fy_n} at its negative regulatory site (Tyr-531). Indeed, NCAM antibodies have been shown to stimulate a tyrosine phosphatase activity in growth cone-enriched membranes (65). The p59^{fy_n} SH2 domain would then become available to bind and recruit p125^{fa_k}. Subsequently, p59^{fy_n} may phosphorylate p125^{fa_k} at additional tyrosine residues that could then recruit other SH2 domain-containing signaling or cytoskeletal proteins. A similar mechanism occurs in nonneuronal cells where antibody-induced ligation or ligand stimulation of integrins by extracellular matrix proteins such as fibronectin increases p125^{fa_k} autophosphorylation on tyrosine residue 397, creating a binding site for p59^{fy_n} or pp60^{c-*src*} (47, 66–68). p125^{fa_k} is then phosphorylated at additional tyrosine residues providing a binding site for Grb2 and activating the Ras-mitogen-activated protein kinase pathway (66, 67, 69). Thus the involvement of p125^{fa_k} in NCAM signaling thus raises the interesting prospect that NCAM may regulate gene transcription. Additionally, p125^{fa_k} is known to recruit the p85 subunit of phosphatidylinositol 3'-kinase (70) and the GTPase-activating protein Graf, a negative regulator of RhoA and Cdc42, which are GTP binding proteins regulating lamellipodial and filopodial formation (71). In another model, p125^{fa_k} may join the NCAM complex indirectly through association with an integrin (72). Although preliminary experiments have not demonstrated an association of NCAM and β_1 -integrin by co-immunoprecipitation from Brij lysates of mouse cerebellum (PND4) or fetal (E18) rat brain, such interactions could be weak or involve another subclass of integrin.

The identification of p125^{fak} as a component of the NCAM140-p59^{syn} complex expands the potential role of the focal adhesion tyrosine kinase from integrin signaling to signal transduction by a cell adhesion molecule of the Ig superfamily. p125^{fak} is expressed in all regions of the central nervous system and is enriched in the growth cones of developing neurons, although its function there has yet to be identified (58, 59). A functional interaction of NCAM and integrins also offers a potential means of convergence of NCAM and integrin-dependent adhesion pathways. Such convergence could provide a means of integrating growth cone guidance cues from extracellular matrix and cell surface adhesion molecules. Such interactions may be permissive for axonal outgrowth or instructive for growth cone guidance at boundaries or guidepost cells. Although p125^{fak} can be activated by clustering of cell surface NCAM140 molecules, it remains to be established whether such activation contributes to axon growth or guidance.

The recent development of *Fak* knockout mice has provided evidence that p125^{fak} functions in regulating focal adhesive contacts induced by integrin binding of extracellular matrix proteins (73). *Fak*-minus mice are impaired in the development of the anterior-posterior axis and in mesodermal structures (73, 74). Inhibition of p125^{fak} by the *Fak*-related nonkinase delays the formation of new focal adhesions (75). Regulated adhesion is expected to be essential for the migration of neuronal growth cones, which establish focal contacts on some substrates but mainly rely upon the making and breaking of transient point contacts during axonal migration (76, 77). Activation of p125^{fak} and p59^{syn} by signaling clusters of NCAM in the growth cone membrane may regulate the dynamics of adhesive contacts, allowing rapid neuronal migration. In nonneuronal cells, p125^{fak} is activated by integrin cross-linking and is recruited to sites of focal contacts on the cell surface together with a host of cytoskeletal and signaling proteins including p59^{syn} (78). In an analogous manner, NCAM140 clustering in the growth cone may recruit and activate not only p125^{fak} but other focal contact-associated cytoskeletal and signaling proteins with net effects on filopodial and lamellipodial dynamics.

Acknowledgments—Dr. Stefan Klinz is gratefully acknowledged for his generous advice and assistance with experiments and many helpful discussions regarding work related to this project. We thank Ron Graff for the NCAM Fc purification, and Terri Worley, Jim Fiordalisi, and Wendy Morse for helpful comments on the manuscript. We are indebted to Drs. Mike Schaller, Shelton Earp, Roger Perlmutter, and Tom Parsons for antibodies and cDNA clones.

REFERENCES

- Cunningham, B. A., Hemperly, J. J., Murray, B. A., Prediger, E. A., Brackenbury, R., and Edelman, G. A. (1987) *Science* **236**, 799–806
- Murray, B. A., Hemperly, J. J., Prediger, E. A., Edelman, G. M., and Cunningham, B. A. (1986) *J. Cell Biol.* **102**, 189–193
- Pollerberg, G. E., Burridge, K., Krebs, K. E., Goodman, S. R., and Schachner, M. (1987) *Cell Tissue Res.* **250**, 227–236
- Persohn, E., Pollerberg, G. W., and Schachner, M. (1989) *J. Comp. Neurol.* **288**, 92–100
- Noble, M., Albrechtsen, M., Moller, C., Lyles, J., Bock, E., Goridis, C., Watanabe, M., and Rutishauser, U. (1985) *Nature* **316**, 725–728
- Rutishauser, U. (1994) *Curr. Opin. Neurobiol.* **3**, 709–715
- Tang, J., Rutishauser, U., and Landmesser, L. (1994) *Neuron* **13**, 405–414
- Small, S. J., Haines, S. L., and Akeson, R. (1988) *Neuron* **1**, 1007–1017
- Liu, L., Haines, S., Shew, R., and Akeson, R. A. (1993) *J. Neurosci. Res.* **35**, 327–345
- Saffell, J. L., Walsh, F. S., and Doherty, P. (1994) *J. Cell Biol.* **125**, 427–436
- Lüthi, A., Laurent, J. P., Figurov, A., Muller, E., and Schachner, M. (1994) *Nature* **372**, 777–779
- Cremer, H., Lange, R., Christoph, A., Plomann, M., Vopper, G., Roes, J., Brown, R., Baldwin, S., Barthels, D., Rajewsky, K., and Wille, W. (1994) *Nature* **367**, 455–459
- Persohn, E., and Schachner, M. (1987) *J. Cell Biol.* **105**, 569–576
- Landmesser, L., Dahm, L., Schultz, K., and Rutishauser, U. (1988) *Dev. Biol.* **130**, 645–670
- Stoeckli, E. T., and Landmesser, L. T. (1995) *Neuron* **14**, 1165–1179
- Atashi, J. R., Klinz, S. G., Ingraham, C. A., Matten, W. T., Schachner, M., and Maness, P. F. (1992) *Neuron* **8**, 1–20
- Klinz, S. G. (1995) *Analysis of Cell Adhesion Molecules L1 and N-CAM in Phosphorylation-mediated Signal Transduction Pathways in Growth Cones from Fetal Rat Brain*. Doctoral dissertation, Swiss Federal Institute of Technology, Zurich
- Doherty, P., Ashton, S. V., Moore, S. E., and Walsh, F. S. (1991) *Cell* **67**, 21–33
- Schuch, U., Lohse, M. J., and Schachner, M. (1989) *Neuron* **3**, 13–20
- von Bohlen und Halbach, F., Taylor, J., and Schachner, M. (1992) *Eur. J. Neurosci.* **4**, 896–909
- Miller, D. R., Lee, G. M., and Maness, P. F. (1993) *J. Neurochem.* **60**, 2134–2144
- Bixby, J. L., and Jhabvala, P. (1992) *J. Neurobiol.* **23**, 468–480
- Williams, E. J., Walsh, F. S., and Doherty, P. (1994) *J. Cell Biol.* **124**, 1029–1037
- Worley, T. L., and Holt, C. E. (1996) *J. Neurosci.* **16**, 2294–2306
- Desai, C. J., Gindhart, J. G. J., Goldstein, L. S. B., and Zinn, K. (1996) *Cell* **84**, 599–609
- Krueger, N. X., Van Vactor, D., Wan, H. I., Gelbart, W. M., Goodman, C. S., and Saito, H. (1996) *Cell* **84**, 611–622
- Beggs, H. E., Soriano, P., and Maness, P. F. (1994) *J. Cell Biol.* **127**, 825–833
- Ignelzi, M. A., Miller, D. R., Soriano, P., and Maness, P. F. (1994) *Neuron* **12**, 873–884
- Fults, D. W., Towle, A. C., Lauder, J. M., and Maness, P. F. (1985) *Mol. Cell Biol.* **5**, 27–32
- Maness, P. F., Aubry, M., Shores, C. G., Frame, L., and Pfenninger, K. H. (1988) *Proc. Natl. Acad. Sci. U. S. A.* **85**, 5001–5005
- Bare, D. J., Lauder, J. M., Wilkie, M. B., and Maness, P. F. (1993) *Oncogene* **8**, 1429–1436
- Grant, S. G. N., O'Dell, T. J., Karl, K. A., Stein, P. L., Soriano, P., and Kandel, E. R. (1992) *Science* **258**, 1903–1910
- Umemori, H., Sato, S., Yagi, T., Aizawa, S., and Yamamoto, T. (1994) *Nature* **367**, 572–576
- Soriano, P., Montgomery, C., Geske, R., and Bradley, A. (1991) *Cell* **64**, 693–702
- Morse, W. R., Whitesides, J. G., Morell, P., LaMantia, A.-S., and Maness, P. F. (1996) *Soc. Neurosci. Abstr.* **22**, 1469
- Stein, P. L., Vogel, H., and Soriano, P. (1994) *Genes Dev.* **8**, 1999–2007
- Schaller, M. D., and Parsons, J. T. (1995) *Mol. Cell Biol.* **15**, 2635–2645
- Lipsich, L. A., Lewis, A. L., and Brugge, J. S. (1983) *J. Virol.* **48**, 352–360
- Cooke, M. P., and Perlmutter, R. M. (1989) *New Biol.* **1**, 66–74
- Martinez, R., Mathey-Prevot, B., Bernards, A., and Baltimore, D. (1987) *Science* **237**, 411–415
- Gauen, L. K. T., Zhu, Y., Letourneur, F., Hu, Q., Bolen, J. B., Matis, L. A., Klausner, R. D., and Shaw, A. S. (1994) *Mol. Cell Biol.* **14**, 3729–3741
- Clark, M. R., Johnson, S. A., and Cambier, J. C. (1994) *EMBO J.* **13**, 1911–1919
- Schubert, D., Heinemann, S., Carlisle, W., Tarikas, H., Kimes, B., Patrick, J., Steinback, J. H., Culp, W., and Brandt, B. L. (1974) *Nature* **249**, 224–227
- Zisch, A. H., D'Alessandri, L., Amrein, K., Ranscht, B., Winterhalter, K. H., and Vaughan, L. (1995) *Mol. Cell Neurosci.* **6**, 263–279
- Thomas, P. M., and Samelson, L. E. (1992) *J. Biol. Chem.* **267**, 12317–12322
- Shenoy-Scaria, A. M., Gauen, L. K. T., Kwong, J., Shaw, A. S., and Lublin, D. M. (1993) *Mol. Cell Biol.* **13**, 6385–6392
- Cobb, B. S., Schaller, M. D., Leu, T.-H., and Parsons, J. T. (1994) *Mol. Cell Biol.* **14**, 147–155
- Kornberg, L. J., Earp, H. S., Turner, C. E., Prockop, C., and Juliano, R. L. (1991) *Proc. Natl. Acad. Sci. U. S. A.* **88**, 8392–8396
- Shattil, S. J., Haimovich, B., Cunningham, M., Lipfert, L., Parsons, J. T., Ginsberg, M. H., and Brugge, J. S. (1994) *J. Biol. Chem.* **269**, 14738–14745
- Chrzanowska-Wodnicka, M., and Burridge, K. (1994) *J. Cell Sci.* **107**, 3643–3654
- Serpente, N., Birling, M.-C., and Price, J. (1996) *Mol. Cell Neurosci.* **7**, 391–403
- Lev, S., Moreno, H., Martinez, R., Canoll, P., Peles, E., Musacchio, J. M., Plowman, G. D., Rudy, B., and Schlessinger, J. (1995) *Nature* **376**, 737–745
- Cheng, S. H., Espino, P. C., Marshall, J., Harvey, R., Merrill, J., and Smith, A. E. (1991) *J. Virol.* **65**, 170–179
- Payne, H. R., Burden, S. M., and Lemmon, V. (1992) *Cell Motil. Cytoskeleton* **21**, 65–73
- Abosch, A., and Lagenaur, C. (1993) *J. Neurobiol.* **24**, 344–355
- Burden-Gulley, S. M., Payne, H. R., and Lemmon, V. (1995) *J. Neurosci.* **15**, 4370–4381
- Williams, E. J., Furness, J., Walsh, F. S., and Doherty, P. (1994) *Neuron* **13**, 583–594
- Burgaya, F., Menegon, A., Menegoz, M., Valtorta, F., and Girault, J.-A. (1995) *Eur. J. Neurosci.* **7**, 1810–1821
- Grant, S. G. N., Karl, K. A., Kiebler, M. A., and Kandel, E. R. (1995) *Genes Dev.* **9**, 1909–1921
- Songyang, Z., Shoelson, S. E., Chaudhuri, M., McGlade, J., Olivier, P., Pawson, T., Bustelo, X. R., Barbacid, M., Sbae, H., Hanafusa, H., Yi, T., Ren, R., Baltimore, D., Ratnofsky, S., Feldman, R. A., and Cantley, L. C. (1994) *Mol. Cell Biol.* **14**, 2777–2785
- Rickles, R. J., Botfield, M. C., Weng, Z., Taylor, J. A., Green, O. M., Brugge, J. S., and Zoller, M. J. (1994) *EMBO J.* **13**, 5598–5604
- Small, S. J., Shull, G. E., Santioni, M.-J., and Akeson, R. (1987) *J. Cell Biol.* **105**, 2335–2345
- Hu, H., Tomasiewicz, H., Magnuson, T., and Rutishauser, U. (1996) *Neuron* **16**, 735–743
- Ono, K., Tomasiewicz, H., Magnuson, T., and Rutishauser, U. (1994) *Neuron* **13**, 595–609
- Klinz, S. G., Schachner, M., and Maness, P. F. (1995) *J. Neurochem.* **65**, 84–95
- Schlaepfer, D. D., Hanks, S. K., Hunter, T., and van der Geer, P. (1994) *Nature* **372**, 786–791
- Calalb, M. B., Polte, T. R., and Hanks, S. K. (1995) *Mol. Cell Biol.* **15**, 954–963
- Eide, B. L., Turck, C. W., and Escobedo, J. A. (1995) *Mol. Cell Biol.* **15**, 2819–2827

69. Chen, Q., Kinch, M. S., Lin, T. H., Burridge, K., and Juliano, R. L. (1994) *J. Biol. Chem.* **269**, 26602–26605
70. Chen, H.-C., Appeddu, P. A., Isoda, H., and Guan, J.-L. (1996) *J. Biol. Chem.* **271**, 26329–26334
71. Hildebrand, J. D., Schaller, M. D., and Parsons, J. T. (1993) *J. Cell Biol.* **123**, 993–1005
72. Schaller, M. D., Otey, C. A., Hildebrand, J. D., and Parsons, J. T. (1995) *J. Cell Biol.* **130**, 1181–1187
73. Ilic, D., Furuta, Y., Kanazawa, S., Takeda, N., Sobue, K., Nakatsuji, N., Nomura, S., Fujimoto, J., Okada, M., Yamamoto, T., and Aizawa, S. (1995) *Nature* **377**, 539–544
74. Furuta, Y., Ilic, D., Kanazawa, S., Takeda, N., Yamamoto, T., and Aizawa, S. (1995) *Oncogene* **11**, 1989–1995
75. Richardson, A., and Parsons, T. (1996) *Nature* **380**, 538–540
76. Arregui, C. O., Carbonetto, S., and McKerracher, L. (1994) *J. Neurosci.* **14**, 6967–6977
77. Gomez, T. M., Roche, F. K., and Letourneau, P. C. (1996) *J. Neurobiol.* **29**, 18–34
78. Miyamoto, S., Teramoto, H., Coso, O. A., Gutkind, S., Burbelo, P. D., Akiyama, S. K., and Yamada, K. M. (1995) *J. Cell Biol.* **131**, 791–805
79. Maness, P. F., Beggs, H. E., Klinz, S. G., and Morse, W. R. (1996) *Perspect. Dev. Neurobiol.* **4**, 159–181